ENGINEERING

Ambient-pressure lignin valorization to high-performance polymers by intensified reductive catalytic deconstruction

Robert M. O'Dea[1]†, Paula A. Pranda[1]†, Yuqing Luo[1]†, Alice Amitrano[1], Elvis O. Ebikade[1,2], Eric R. Gottlieb[1], Olumoye Ajao[3], Marzouk Benali[3], Dionisios G. Vlachos[1,2], Marianthi Ierapetritou[1,2], Thomas H. Epps, III[1,4,5]*

Chemocatalytic lignin valorization strategies are critical for a sustainable bioeconomy, as lignin, especially technical lignin, is one of the most available and underutilized aromatic feedstocks. Here, we provide the first report of an intensified reactive distillation–reductive catalytic deconstruction (RD-RCD) process to concurrently deconstruct technical lignins from diverse sources and purify the aromatic products at ambient pressure. We demonstrate the utility of RD-RCD bio-oils in high-performance additive manufacturing via stereolithography 3D printing and highlight its economic advantages over a conventional reductive catalytic fractionation/RCD process. As an example, our RD-RCD reduces the cost of producing a biobased pressure-sensitive adhesive from softwood Kraft lignin by up to 60% in comparison to the high-pressure RCD approach. Last, a facile screening method was developed to predict deconstruction yields using easy-to-obtain thermal decomposition data. This work presents an integrated lignin valorization approach for upgrading existing lignin streams toward the realization of economically viable biorefineries.

INTRODUCTION

Lignocellulosic biomass (LCB) is the most abundant form of biomass on Earth, and its valorization has been studied extensively for producing sustainable fuels, chemicals, and materials (*1*–*8*). The composition of LCB is approximately 40 to 60% cellulose, 10 to 40% hemicellulose, and 15 to 30% lignin (*9*), and the specific percentages depend on the type of biomass (*1*). Cellulose and hemicellulose are polysaccharides that are readily converted into fuels and chemicals, such as hydroxymethylfurfural or sugar alcohols such as xylitol, through straightforward acid catalysis (*5*, *10*), while lignin is a complex aromatic polymer network whose valorization is challenging because of its inherent recalcitrance (*1*, *5*). Presently, lignin is separated from biomass at a rate of approximately 70 to 100 million metric tons/year through pulping or biorefining processes (*11*, *12*), but most isolated lignins have a dark color, strong odor, broad molecular weight distribution, and limited reactivity (*5*, *13*–*15*), which restricts them to low-value applications (e.g., fillers for tires, asphalt, or concrete) (*16*, *17*). Furthermore, there is substantial variability in the composition, chemical structure, cost, and environmental impact of technical lignins due to differences among feedstocks and pulping/refining techniques (*13*, *18*–*20*).

Lignin deconstruction or depolymerization is a promising valorization approach for technical lignin, as it can generate products much more valuable than bulk lignin (*1*, *2*, *4*, *5*, *21*, *22*). Reductive catalytic deconstruction (RCD) and reductive catalytic fractionation (RCF) are particularly promising strategies that deconstruct lignin into its phenolic constituents at high yields, with the RCF process also incorporating a simultaneous LCB fractionation step (*1*, *23*–*27*). RCF or RCD typically uses a supported metal catalyst and an alcohol solvent (e.g., methanol or ethanol) to concurrently dissolve the lignin and deconstruct it at ~200° to 250°C (Fig. 1A) (*1*). Hydrogen gas often is added under pressure to promote hydrogenation over lignin recombination by "capping" reactive species; however, the alcohol solvent also can act as a hydrogen donor to avoid these recondensation

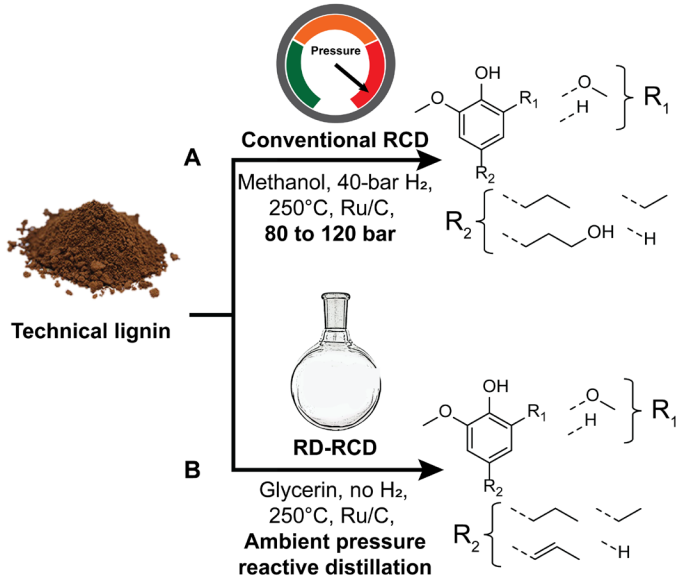

Fig. 1. Overview of RCD processes. (**A**) Conventional RCD using methanol as a solvent, 40-bar external H_2, and 5 weight % (wt%) Ru/C as a catalyst and (**B**) RD-RCD developed in this work using glycerin as a solvent and no external H_2. At an operating temperature of 250°C, conventional RCD is pressurized to between 80 and 120 bar, whereas RD-RCD operates at ambient pressure.

[1]Department of Chemical and Biomolecular Engineering, University of Delaware, Newark, DE 19716, USA. [2]Catalysis Center for Energy Innovation, 221 Academy St., Newark, DE 19716, USA. [3]Natural Resources Canada, CanmetENERGY, P.O. Box 4800, Varennes, Quebec J3X 1S6, Canada. [4]Department of Materials Science and Engineering, University of Delaware, Newark, DE 19716, USA. [5]Center for Research in Soft matter and Polymers (CRiSP), University of Delaware, Newark, DE 19716, USA.
†These authors contributed equally to this work.
*Corresponding author. Email: thepps@udel.edu

reactions (*24*, *28*). A major drawback of current RCF/RCD-based techniques is the use of volatile, flammable solvents at high temperatures and pressures, resulting in significant safety hazards, high capital costs, and considerable energy requirements (*29*). Furthermore, high-pressure reactions typically are restricted to batch processing and have a limited throughput for a given system size, resulting in higher unit operation costs (*29*, *30*). Comparatively, low-pressure RCF/RCD has been reported in less volatile solvents (e.g., ethylene glycol) (*24*, *31*), but there are still solvent toxicity and sustainability challenges with these low-volatility alcohols (*32*, *33*). We note that the conventional RCF and conventional RCD process conditions are identical in this work; however, we use RCD going forward because the technical lignin specimens do not require the standard LCB fractionation step.

Here, we report an intensified reactive distillation (RD)–RCD process (see Fig. 1B) that uses glycerin, an inexpensive, sustainable, and low-volatility by-product of biodiesel production, as the solvent. The high boiling point of glycerin (~290°C) enables ambient-pressure operation, along with simultaneous RD for more efficient separation of phenolic deconstruction products. Although RCF-type processes typically are used in lignin-first valorization strategies, this work focuses on the valorization of technical lignins obtained from common pulping methods and uses conventional RCD in methanol as a benchmark for deconstruction efficiency. The phenolic deconstruction products were functionalized with photopolymerizable acrylate groups, incorporated into a photocurable three-dimensional (3D) printing resin for additive manufacturing, and printed using a commercially available stereolithography (SLA) 3D printer. Furthermore, technoeconomic analysis (TEA) for both conventional and RD-RCD illustrated the effect of the process intensification and lignin source on economics for the production of a pressure-sensitive adhesive (PSA). Overall, the RD-RCD process improved the deconstruction efficiency versus RCD and resulted in more cost-competitive bioproducts. Last, a fast and inexpensive lignin screening method was established to predict deconstruction yields from thermal degradation behavior, providing a streamlined alternative to bench-scale RCD-type experimentation or ^{31}P nuclear magnetic resonance (NMR) spectroscopy to assess the economic feasibility of technical lignin valorization.

RESULTS AND DISCUSSION

Reactive distillation–reductive catalytic deconstruction

RD-RCD and conventional RCD were used to deconstruct technical lignins obtained via Kraft, organosolv, soda, and thermomechanical pulping processes. A summary of the lignin feedstocks is shown in Table 1. Phenolic product yields [weight % (wt%) on a lignin basis] for both processes with different technical lignins are provided in Fig. 2. Conventional RCD resulted in yields ranging from 4.7 to 45.6%, whereas RD-RCD yields were between 8.3 and 31.7%. RD-RCD also generated solvent reforming by-products, such as substituted dioxolanes, solketal, and cyclopentenones, that were collected in the extracted distillate. These secondary products accounted for between 45 and 76% of the product mixture, depending on the lignin feedstock. Gas chromatography–mass spectrometry (GC-MS) plots, method validation, a representative mass balance, and yields for a catalyst-free control experiment are shown in figs. S1 to S9 and tables S1 to S4.

The intensified RD-RCD provides several benefits over conventional RCD. Specifically, operating at ambient pressure overcomes a key scale-up hurdle, reduces capital requirements, and mitigates safety hazards (*29*). The use of glycerin is also advantageous because it is environmentally benign and is obtained as a by-product of biodiesel production (*34*). Additionally, RD-RCD simplifies product purification and reduces energy intensity because a cooling step is not required before extracting phenolic products in contrast to conventional RCD (*6*). The yields for both processes were comparable for most samples; however, conventional RCD resulted in higher phenolic product yields than RD-RCD for more "deconstructable" lignins (e.g., BHF, biorefinery hardwood filtration), whereas the reverse was true for more recalcitrant lignins (e.g., KSA, Kraft softwood CO_2 acidification). The concurrent removal of phenolic products through distillation as they form may have driven these differences in yields between the two processes; however, further studies are needed to elucidate the underlying reaction mechanisms and confirm this hypothesis.

The two processes generated bio-oils with varying product distributions. As expected, softwood lignin (sample KSA) yielded almost exclusively guaiacyl (G) units; hardwood lignins (samples KHA1, Kraft hardwood CO_2 acidification1, KHA2, Kraft hardwood CO_2 acidification2, OHP, organosolv hardwood solvent precipitation, and BHF) produced a mixture of G and syringyl (S) compounds; and herbaceous lignin (sample SNWA, soda nonwood mineral acidification) formed *p*-hydroxyphenyl (H), G, and S units. The RCD products generally contained larger amounts of S compounds than RD-RCD because S units are less volatile than H and G compounds and do not distill completely in RD-RCD. For instance, the selectivity of S compounds (i.e., the sum of the selectivities of S-type compounds) generated from sample BHF was 74% for RCD, whereas this value was 22% for RD-RCD. This behavior potentially accounts for the differences

Table 1. Lignin samples and key characteristics.

Sample	Process type	Biomass type	Precipitation method	Region	Species
KHA1	Kraft	Hardwood	CO_2 acidification	South America	Eucalyptus
KSA	Kraft	Softwood	CO_2 acidification	Europe	Pine
SNWA	Soda	Nonwood	Mineral acidification	Asia	Wheat straw
KHA2	Kraft	Hardwood	CO_2 acidification	Europe	Birch
OHP	Organosolv	Hardwood	Solvent precipitation	Europe	Beech
BHF	Biorefinery	Hardwood	Filtration	North America	Birch

in yields between RD-RCD and RCD for samples that generated comparatively large amounts of S compounds via RCD, such as BHF and OHP. The identified phenolic compounds and their respective selectivities (i.e., the proportion of all detected phenolic compounds) for each technical lignin are shown in Fig. 3.

Beyond the proportions of H, G, and S products, the substituent groups at the 4-position varied depending on the process and the type of lignin. The substitutions common to lignin oils from both RD-RCD and RCD were hydrogen, methyl, ethyl, and propyl chains, and in the case of RD-RCD, some propenyl and vinyl moieties were generated. Conventional RCD also produced hydroxypropyl-substituted phenolics. Between the two deconstruction approaches, RCD generated higher amounts of propyl-substituted phenolics, whereas RD-RCD resulted in compounds with shorter alkyl chains or no 4-substitution. This trend is most apparent with sample KSA; the selectivity for propylguaiacol was 48% for RCD, and the selectivity for guaiacol was 57% for RD-RCD. Among the different pulping methods, Kraft lignins (KHA1, KSA, and KHA2) produced greater amounts of unsubstituted compounds (e.g., guaiacol and syringol), and soda, biorefinery, and organosolv lignins (i.e., lignins from milder pulping/fractionation techniques) resulted in bio-oils rich in propyl substituents. For instance, the selectivity for propyl-substituted phenolics was 64% for BHF RD-RCD bio-oil and only 12% for KHA1 RD-RCD bio-oil. Pulping and deconstruction methods significantly affect selectivities within the group of shared RCD/RD-RCD products, and the relationship between the feedstock (biomass type and separation method), deconstruction technique, and product selectivities could be leveraged to tailor the slate of biobased chemicals generated in a biorefinery.

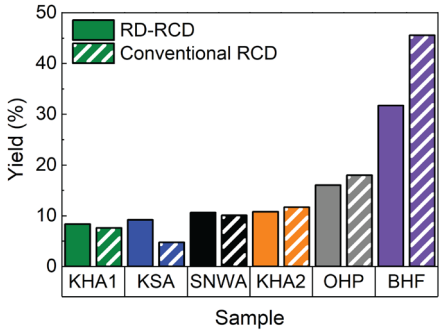

Fig. 2. Comparison of RD-RCD and RCD deconstruction yields. RD-RCD phenolic product yields (solid) and conventional RCD phenolic product yields (striped) for six lignin samples. All reactions were run for 15 hours at 250°C.

Additionally, RD-RCD generates compounds with unsaturated substituents and solvent reforming by-products that are absent in conventional RCD conducted with external H_2. For instance, isoeugenol, propenylsyringol, and vinylguaiacol are present in RD-RCD distillates but not in the conventional RCD bio-oils. Products with unsaturated functional groups likely are generated because RD-RCD removes them via distillation, whereas in conventional RCD, the products undergo further hydrogenation. However, note that conventional RCD can be altered to generate more unsaturated products by eliminating external H_2 or removing the catalyst altogether at the expense of reduced yields (*24*, *35*, *36*). Among the lignin samples, those from harsher pulping processes, such as sample KSA, produced the lowest amount of unsaturated compounds in RD-RCD (1.4% of the phenolic products), and lignins from gentle processes, such as sample BHF, had the highest proportion of unsaturated products (11.4%), which can be rationalized on the basis of acid content in the feedstocks (*37*, *38*). Varying levels of glycerin decomposition/reforming compounds, including cyclopentanones, cyclopentenones, solketal, and dioxolanes, were also detected in all RD-RCD bio-oils (see figs. S1 to S7 and table S1). These reforming products are generated even in the absence of lignin (fig. S10). The boiling points of these chemicals generally are lower than those of the phenolic products

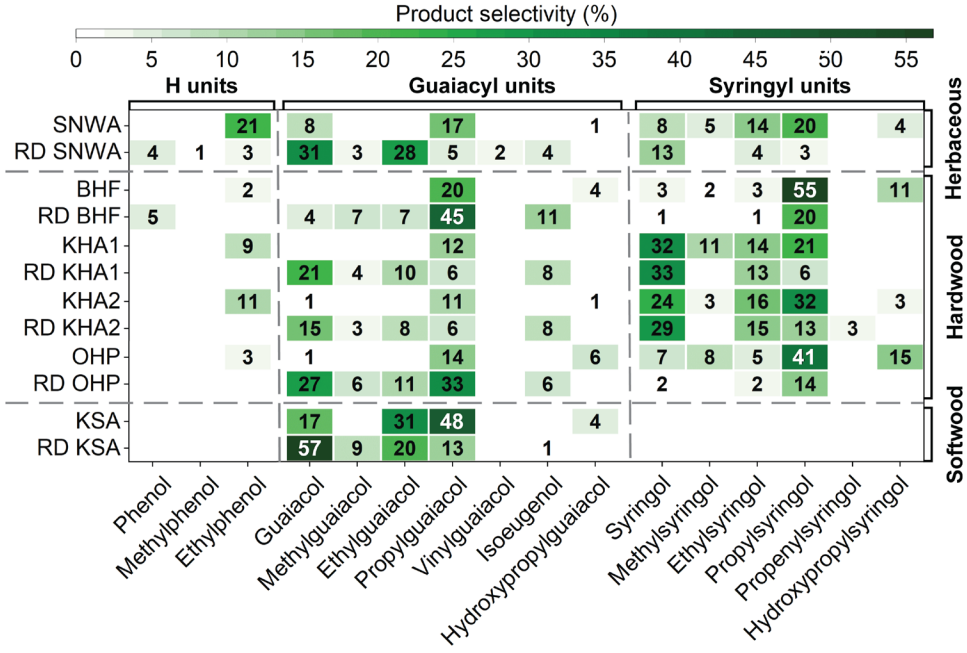

Fig. 3. Product selectivities for phenolic RCD and RD-RCD products. The sample name indicates conventional RCD (e.g., KSA), and RD indicates reactive distillation (e.g., RD KSA). Dashed lines separate feedstock type (horizontal lines) and lignin subunit type (vertical lines). Selectivities above 40% are shown in white text for clarity.

(~150°C versus >200°C) such that they could be separated via distillation. Alternatively, condensed-phase (e.g., chromatographic) methods could be used to further improve economics and reduce the environmental impact of the process in comparison to distillation (*30*). The purified compounds then could be treated as co-products with applications as platform chemicals or green solvents. For example, cyclopentenones are valuable precursors for pharmaceuticals and fragrances (*39*).

Biobased 3D printing

RCF/RCD deconstruction products or "bio-oils" have been used as precursors for numerous bio-derived products, such as polymers and pharmaceuticals (*6*, *35*, *40*), and the generation of biobased materials from RCF/RCD oils is particularly attractive, as it can minimize the need for significant product purification (*5*, *6*). Additive manufacturing is gaining traction within the biobased materials space as a versatile fabrication approach (*3*, *4*, *41*), and SLA 3D printing is a technique that uses visible or ultraviolet light to photocure resins (*42*). Lignin and lignin-derivable compounds have been incorporated into photocurable resins; however, to the authors' knowledge, the use of RCF/RCD oil mixtures for SLA printing has not been reported (*3*, *41*, *43*). Furthermore, most SLA resins are composed of alkyl methacrylates, and translating biobased, lignin-derived monomers to 3D printing resins offers a new class of materials for additive manufacturing.

To demonstrate the utility of RD-RCD lignin oils, acrylated SNWA bio-oil was incorporated into an SLA resin and 3D printed using a commercially available printer. SNWA bio-oil was chosen because it had a high syringol content and was produced from sulfur-free lignin. The complete 3D printing formulation contained 40 wt% acrylated bio-oil obtained directly from the RD-RCD products generated in this work, 40 wt% lignin-derivable vanillyl alcohol diacrylate, 15 wt% Peopoly resin, and 5 wt% photoinitiator. The diacrylate and Peopoly resin were added to improve overall print quality (fig. S11). The acrylation reaction and a photo of a printed object from our formulation are shown in Fig. 4. A second resin was prepared from the acrylated bio-oil and vanillyl alcohol diacrylate without Peopoly resin, and the material was cured following the same procedure. However, the print without Peopoly exhibited breaking/flaking after several minutes (fig. S11).

The printed SLA resin is a salient example of the multiple potential applications for RD-RCD bio-oils and other co-products. The material properties (e.g., glass transition temperature and solvent resistance) can be tuned by leveraging structure-property relationships (*5*, *6*, *44*–*47*) to choose mixtures of bio-oils from different feedstocks for a target monomer composition. Furthermore, formulation for SLA printing required the addition of a cross-linker because inert (i.e., non-acrylated) components in the bio-oil mixture solvated the polymer and prevented the formation of a solid print, although polymers from the phenolic acrylates are expected to be in a glassy state at room temperature (*6*). This behavior demonstrates the potential utility of the glycerin reforming by-products as green solvents and presents an exciting opportunity for further process intensification by avoiding the separation of functionalized monomers and inactive by-products using energy-intensive methods such as distillation.

TEA of lignin-based PSA production

RCD and RD-RCD were compared using a biobased PSA as an example product. The PSA was chosen over SLA printing resins because the market is more mature and higher in volume than the 3D printing resin market. The adhesive market was estimated at $52.6 billion in 2017 and is projected to grow at 5.6% annually through 2025, with PSAs accounting for ~27% of the revenue (*48*). In a previous study, a triblock polymer PSA synthesized by Wang *et al.* (*6*) using a poplar wood RCF oil exhibited superior adhesive performance in comparison to incumbent commercial products when evaluated via American Society for Testing and Materials (ASTM) standard tests, even without added tackifiers. Given the high performance and versatility of this biobased PSA, a similar triblock polymer was used for TEA in this work.

The lignin deconstruction yields and product distributions obtained from the conventional and RD-RCD experiments were used to design two lignin-based PSA production processes in Aspen Plus V11 (Aspen Technology) (*49*, *50*), starting with the RCD or RD-RCD deconstruction reactions and followed by purification, functionalization, and polymerization. Additional details are included in the Supplementary Materials (table S5 and fig. S12), and process flow diagrams are provided in figs. S13 to S15. The lignin capacity of each system was assumed to be 18,144 metric tons/year as a base case. First, lignin was deconstructed by RCD or RD-RCD to produce a mixture of phenolic compounds at 250°C. In the case of RD-RCD, solvent

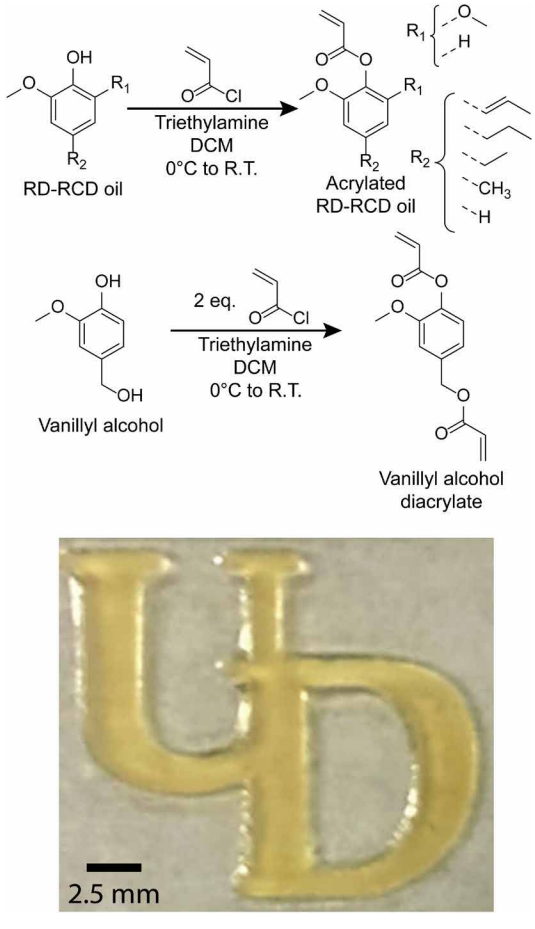

Fig. 4. SLA 3D printing. (**Top**) Functionalization reactions for RD-RCD bio-oil and vanillyl alcohol. (**Bottom**) 3D printed UD using the SLA resin in a commercially available SLA printer. The photo was taken after rinsing with isopropanol and post-curing under an ultraviolet lamp for 10 min. R.T., room temperature.

reforming by-products also were generated, which were assumed to be sold as fuel. In both RCD and RD-RCD, the phenolic products required further purification by liquid-liquid extraction with hexane. For RCD, the extraction separated the phenolic compounds from the residual lignin and lignin oligomers. In RD-RCD, the extraction served to isolate the phenolic products in the distillate from hydrophilic by-products and glycerin. After extraction, the phenolic mixtures were functionalized using methacrylic anhydride (MAAH) with 4-dimethylaminopyridine (DMAP) as a catalyst at 45°C. The residence time for the functionalization reaction was 3 hours to ensure complete conversion. Next, quicklime (CaO) was used to neutralize the unreacted MAAH and methacrylic acid (MAA) by-product. Then, the functionalized acrylic monomers were extracted from the aqueous phase with anisole. The extracted monomers were copolymerized with butyl acrylate (BA) by reversible addition-fragmentation chain transfer (RAFT) polymerization in anisole at 70°C using butan-2-one-3-ethyltrithiocarbonate as the chain transfer agent (CTA) and 2,2′-azobis(isobutyronitrile) as the initiator (*6*). After polymerization, the anisole was removed under reduced pressure to obtain the PSA polymer.

Three representative lignin samples (KSA, OHP, and BHF) were considered in this analysis, and because the biobased PSA polymer's market price is unknown, the minimum selling price (MSP) was chosen as the metric to compare the production costs. The most significant driver was the deconstruction yield, as illustrated in Fig. 5, figs. S16 and S17, and tables S6 to S12. For instance, with KSA lignin, RD-RCD generated PSA polymer at 1202 kg/hour and solvent reforming by-product at 271 kg/hour, and RCD produced PSA at just 592 kg/hour. The low throughput of RCD resulted in a MSP of $20,732/t, whereas the comparatively higher throughput of RD-RCD enabled a 62% lower MSP of $7901/t, as shown in Fig. 5, A and B. The differences between the two processes were less pronounced for other lignin samples. RD-RCD outperformed RCD in all cases, even when RD-RCD yields were lower. For example, the RCD PSA production rate for BHF was significantly higher than that for RD-RCD, 3545 kg/hour versus 2478 kg/hour, but the MSP was $6440/t for RCD in comparison to $6163/t for RD-RCD (Fig. 5, C and D) because the glycerin reforming by-products from RD-RCD can be sold as biofuel. Similarly, with OHP lignin, RCD and RD-RCD generated PSA at 2030 and 1845 kg/hour, respectively, leading to MSPs of $8773/t and $7067/t (figs. S16 and S17).

The RD-RCD process exhibited improved unit economics in comparison to conventional RCD, particularly in the deconstruction stage. The solvent reforming by-product biofuel revenue and significantly lower capital requirement for the reactor were the primary drivers of the favorable economic performance (Fig. 6A). Both processes had the same plant configuration for the functionalization and polymerization stages, and because the expenses at this stage are dominated by the raw material costs, including MAAH and BA (Fig. 6A), the contributions of these operations to the MSP are comparable for both systems and nearly independent of the deconstruction yields.

The TEA also provided insights into future cost-saving and revenue-generating opportunities. The most efficient approach to reduce the cost of the deconstruction stage for both RCD and RD-RCD is to reduce the capital requirements, especially the cost of the deconstruction reactors. This goal could be achieved by optimizing

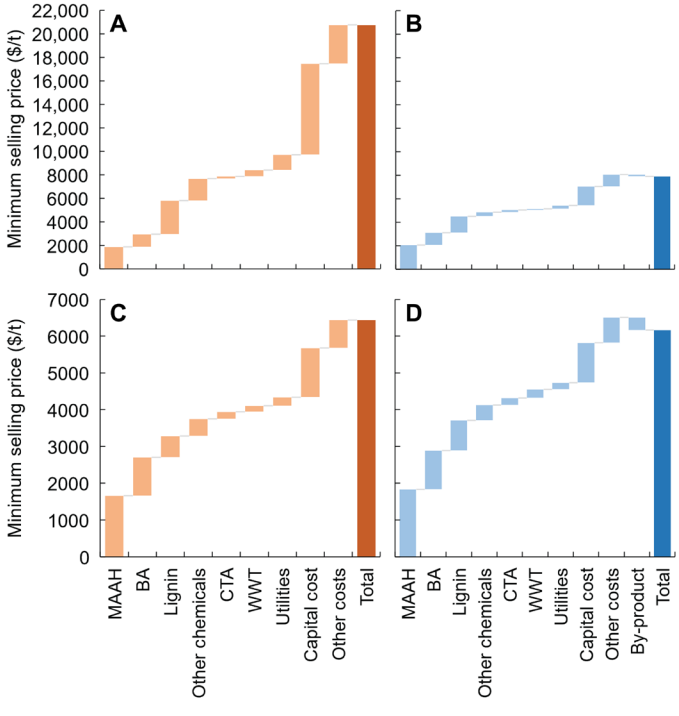

Fig. 5. MSP breakdown for different feedstocks. (**A**) RCD with KSA lignin feedstock. (**B**) RD-RCD with KSA lignin feedstock. (**C**) RCD with BHF lignin feedstock. (**D**) RD-RCD with BHF lignin feedstock. WWT, wastewater treatment.

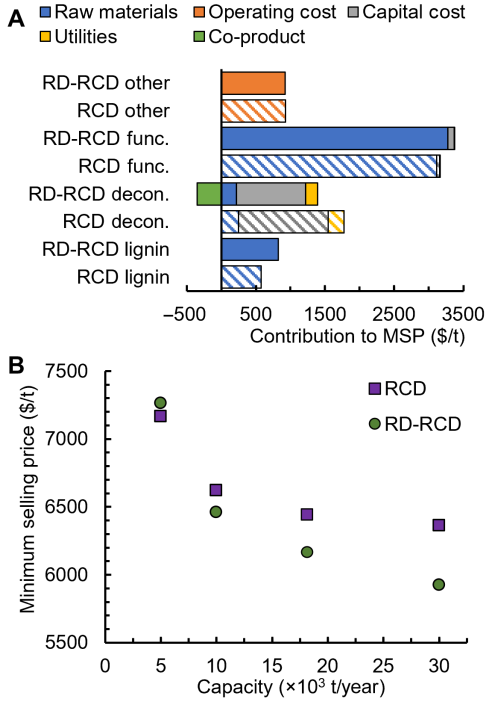

Fig. 6. Contribution of process stages to MSP and impact of plant capacity. (**A**) Economic contribution of process stages to the MSP for RD-RCD (solid) and RCD (striped) using BHF lignin at a scale of 18,144 t/year. Raw materials for each stage did not include the products from the previous stage; for instance, the phenolic compounds from RCD were not included in the raw material cost for the functionalization step. (**B**) MSP of PSA relative to plant capacity for RCD (purple squares) and RD-RCD (green circles) using BHF lignin. func., functionalization; decon., deconstruction (A).

the catalyst and reaction conditions to reduce the reaction time and solvent consumption. Lowering raw material costs also would have a substantial impact on process economics. For instance, the cost of MAAH is a leading contributor to the MSP, and converting the MAA back to MAAH would significantly reduce the final PSA price (*51*). Additionally, expanded implementation of commercial lignin recovery technologies will increase the supply of lignin and likely contribute to reduced feedstock costs and MSPs. Plant economics also could be drastically improved by generating saleable products from the residual, partially deconstructed lignin. In this work, the residual lignin is considered waste to simplify the comparison between RCD and RD-RCD; however, as technical lignins tend to be somewhat recalcitrant, this stream accounts for most of the input lignin feedstock. Oligomeric lignin has been used in numerous materials applications (*27*, *52*–*56*), and it is possible to recover this partially deconstructed lignin through precipitation for further upgrading (see fig. S9 and table S3).

The economic impact of the chemical plant capacity was evaluated using BHF lignin feedstock capacities ranging from 5000 to 30,000 t/year in a sensitivity analysis (Fig. 6B). With an increase in plant capacity to 30,000 t/year, the MSPs of both RCD and RD-RCD PSAs were reduced to $6362/t and $5924/t, respectively. At this scale, the MSP of the RD-RCD PSA was lower than that of RCD, even without selling the solvent reforming by-products as fuel. However, at a significantly smaller scale, such as 5000 t/year, RCD and RD-RCD had comparable MSPs of $7167/t and $7264/t, respectively. Furthermore, the economic impact of plant capacity was more pronounced for RD-RCD than conventional RCD, and thus, the scale-up advantages of RD-RCD are more substantial. Additional sensitivity analyses were performed using other process parameters, as shown in figs. S18 and S19, with more details provided in the Supplementary Materials.

Overall, RD-RCD was economically favorable with all three of the feedstocks included in this analysis. For lignins with lower yields, such as KSA lignin, the benefits of RD-RCD were more pronounced than for lignins with higher deconstruction yields (e.g., BHF). MSPs generally were in the range of $6000/t to $8000/t and are thus competitive with incumbent commercial PSAs. Key parameters for process economics were plant size, solvent consumption, energy usage, and operation mode (batch versus continuous).

Technical lignin screening method

Lignin deconstruction yields had a significant impact on process economics, and thus, simple screening methods to assess the "deconstructability" of technical lignins are needed to determine the economic viability of valorization approaches. To this end, RCD phenolic yields from both conventional RCD and RD-RCD were used to develop an empirical relationship to predict phenolic yields with thermal degradation characteristics measured by thermogravimetric analysis (TGA). Each sample exhibited a characteristic TGA decomposition peak (%/°C), and the temperature at which 40% mass loss occurred ($T_{40\%}$) indicated a point just after the peak for all samples (*57*). Lignin phenolic product yields (on a lignin basis) were plotted against $T_{40\%}$ and fit to exponential functions using least squares. The experimental data and exponential fits for RD-RCD and RCD are shown in Fig. 7 (A and B, respectively), and TGA curves are shown in figs. S20 to S25. Similarly, RD-RCD and RCD yields were correlated with the amount of condensed phenolic units as determined by ^{31}P NMR spectroscopy (figs. S26 to S31 and table S13), as shown in Fig. 7 (C and D).

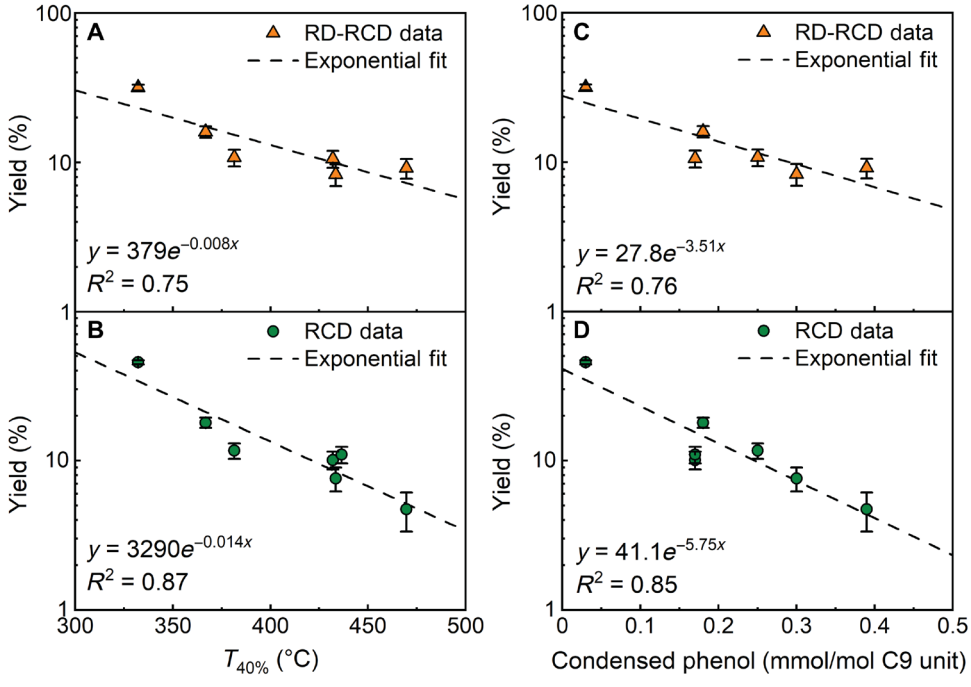

Fig. 7. Screening method for technical lignin feedstocks. (**A**) RD-RCD phenolic yields versus $T_{40\%}$ (from TGA). (**B**) RCD phenolic yields versus $T_{40\%}$. (**C**) RD-RCD phenolic yields versus condensed phenol content (from ^{31}P NMR spectroscopy). (**D**) RCD phenolic yields versus condensed phenol content. Experimental data (RD-RCD: orange triangles; RCD: green circles) and an exponential fit (dashed lines) are shown on logarithmic scales. The exponential fits to deconstruction yields and $T_{40\%}$ had R^2 values of 0.87 and 0.75 for RCD and RD-RCD, respectively. The fits to deconstruction yields using condensed phenol content were of similar quality, with R^2 values of 0.85 and 0.76, respectively.

The inverse correlation of deconstruction yield and $T_{40\%}$ arises from the distribution of interunit linkages; lignins with higher thermal stabilities contain more recalcitrant bonds, whereas lignins with relatively low thermal stabilities contain more labile linkages that are more easily broken during RCD or RD-RCD. The effect of thermal stability on yield was stronger for conventional RCD in comparison to RD-RCD (Fig. 7, A and B), likely because RD-RCD removed phenolic products as they formed and prevented recondensation, whereas RCD relies on hydrogenation to mitigate condensation reactions. Condensed phenol content also was correlated with RCD yield for both processes to serve as a benchmark (Fig. 7, C and D), and the two correlations were of similar quality, as suggested by comparable R^2 values (Fig. 7). Although the correlations are comparable, the condensed phenol metric necessitated using previously reported ^{31}P NMR spectroscopy data from experiments that were comparatively more complex than was TGA (*58*). For instance, lignin samples first were phosphorylated for NMR spectroscopy analysis, whereas no pretreatment was needed for TGA (*58*). Thus, the development of the TGA-based correlation enables facile screening of potential technical lignin feedstocks for RCD valorization strategies with a level of accuracy comparable to the more complex NMR spectroscopy method. This correlation is currently limited to technical lignins because cellulose, hemicellulose, extractives, and other biomass components may lead to more complex thermal decomposition profiles. Despite this constraint, this method to predict deconstruction yields via TGA can screen technical lignin samples for compatibility with other lignin valorization processes, such as biological, pyrolytic, and other catalytic valorization approaches.

In summary, RD-RCD is introduced to simultaneously fractionate biomass, deconstruct lignin, and distill the phenolic products at ambient pressure. It enables facile scale-up and product separations compared to conventional lignin-first fractionation/deconstruction strategies, mitigates safety hazards associated with high-pressure RCF/RCD, and eliminates the energy-intensive H_2. It also replaces alcohol solvents with glycerin, a more environmentally friendly, inexpensive, and abundant by-product of biodiesel production. The RD-RCD bio-oil was functionalized and incorporated into an ~80% biobased resin and printed successfully with a commercially available SLA 3D printer, illustrating the utility of these lignin-derived mixtures in high-performance materials applications. TEA for the production of a PSA demonstrated that RD-RCD provides favorable MSPs compared to traditional RCD for three different technical lignin feedstocks, with as much as a 60% reduction for softwood Kraft lignin. Last, we introduced a straightforward, fast, and inexpensive thermal decomposition method for screening potential feedstock candidates. Together, this work demonstrates the potential of technical lignin as an inexpensive and abundant resource for producing value-added chemicals and materials and a scalable valorization pathway for feedstock selection, intensified deconstruction, product fabrication, and economic evaluation.

MATERIALS AND METHODS

Materials

Glycerin [99%, American Chemical Society (ACS) grade], methanol (>99%, ACS grade), dichloromethane (DCM; 99%), isopropanol (ACS grade), Irgacure TPO-L, and 5 wt% ruthenium on carbon (Ru/C; powder, reduced) were purchased from Fisher Scientific. Acryloyl chloride (96%) and vanillyl alcohol were purchased from Sigma-Aldrich. Peopoly Moai model resin (green) was purchased from MatterHackers (Lake Forest, CA). All reagents were used as received. Technical lignins were provided by Natural Resources Canada–CanmetENERGY and used as received.

Methods

Conventional RCD

RCD in methanol was conducted according to previous studies (*6*). Technical lignin (200 mg), methanol (20 ml), and Ru/C (100 mg) were loaded into a 25-ml Parr reactor. The reactor was sealed, purged three times with nitrogen, pressurized to 40 bar with H_2, and heated to 250°C. The reaction was allowed to proceed for 15 hours before cooling to ambient temperature. Then, the reactor was opened to the atmosphere, and the contents were filtered to remove insoluble residues in addition to the catalyst powder. The filtered solids were rinsed with methanol to recover any residual products, and the alcoholic wash solution was combined with the filtrate. Methanol was removed by rotary evaporation, yielding a dark, viscous oil. This RCD process served as a benchmark for comparison with RD-RCD.

Reactive distillation–reductive catalytic deconstruction

Technical lignin (4 to 5 g) and glycerin (125 ml) were loaded into a 250-ml glass, round-bottom flask equipped with a Teflon magnetic stir bar. Ru/C powder was loaded in a ~2:1 lignin-to-catalyst weight ratio. A distillation apparatus (distillation adapter and receiving flask) was attached using an elbow adapter with a vacuum takeoff (open to atmosphere to prevent pressurization) to connect the receiving flask. The reactor then was heated to 250°C using a DrySyn block on an IKA RCT Basic hot plate with a PT1000 thermocouple. The reaction was allowed to proceed for 15 hours before cooling to room temperature. The unrefined distillate was extracted with DCM (ethyl acetate could serve as a more sustainable alternative) to separate the phenolics from glycerin and other DCM-insoluble products that carried over to the receiving flask. After phase separation in a separatory funnel, the DCM was removed by rotary evaporation to yield an amber RD-RCD bio-oil.

RCD product analysis

RCD oils were analyzed by GC-MS using an Agilent 7890B series gas chromatograph equipped with an HP-5 capillary column and an Agilent 5977A series MS detector with helium as the carrier gas. The injection temperature was 250°C, and the initial column temperature was 50°C. After 1 min at 50°C, the column temperature was ramped to 300°C at 15°C/min and then held at 300°C for 7 min. The detector temperature was set to 290°C. Products were identified using the National Institute of Standards and Technology (NIST) mass spectrum library in Agilent's MassHunter software. Product distributions and yields were quantified with the same gas chromatograph series equipped with a flame ionization detector (GC-FID) using helium as the carrier gas. The injection temperature was 300°C. The column temperature was held at 40°C for 3 min and ramped to 100°C at 30°C/min, followed by a ramp (40°C/min) to 300°C and a 5-min hold. The FID temperature was 300°C. Yields and product selectivities were determined using an internal standard, *n*-decane, and an effective carbon number approach from previous studies (*35*).

RD-RCD product analysis

RD-RCD distillates were analyzed by GC-MS (Agilent 6890 gas chromatograph with a 5973 MS detector and HP-5 column using helium as the carrier gas) to identify products. Identifications were made using the NIST mass spectral library and mass spectra of pure

reference compounds (fig. S1 and table S2). The injection temperature was 250°C, and the column temperature initially was set to 70°C. The column temperature was held at 70°C for 1 min. Then, the temperature was ramped at 10°C/min to 280°C and held for 6 min. By-products co-eluted with the *n*-decane standard, so GC-FID analysis was not possible. Instead, GC-MS was used to quantify the product distributions using peak areas, and the total fraction of phenolic products (i.e., the sum of identified phenolic peak areas normalized by total peak area) was used in conjunction with the overall DCM-extracted distillate mass to determine yields. Additional information regarding data analysis is provided in the Supplementary Materials, and RD-RCD oil chromatograms are shown in figs. S2 to S7. This GC-MS method was semiquantitative but sufficient for this analysis (see fig. S8 and table S2) (*59*).

SLA printing

A digital 3D model of UD lettering was built using the Fusion 360 (version 2.0.8407) software by Autodesk. The model was converted to a G-code file for the printer using Peopoly's Asura 3D (version 2.2.2) software. To prepare a printable resin, nonwood, acid-precipitated soda lignin (SNWA) bio-oil was functionalized with polymerizable acrylate groups using a procedure adapted from (*6*). Vanillyl alcohol diacrylate (40 wt%; prepared with a similar acrylation scheme) and Peopoly resin (15 wt%) were added to the acrylated bio-oil as cross-linkers, and Irgacure TPO-L (5 wt%) was used as the photoinitiator, resulting in a formulation with 40 wt% of the biobased RD-RCD products generated using the approach described herein, 40 wt% lignin-derivable diacrylate, and 20 wt% commercially sourced components. The resin was printed on a glass slide using a Peopoly Moai 200 SLA printer with a 150-mW, 405-nm laser. The laser power was reduced to 45 mW to minimize shrinkage of the resin upon curing, and the glass microscope slide was used as an alternative to the printer vat to minimize material consumption. The print was rinsed with isopropanol for ~5 min before post-print curing under an ultraviolet lamp (Peopoly, 60 W, 405 nm) for 10 min at room temperature. A second biobased resin was prepared from the acrylated bio-oil (50 wt %), vanillyl alcohol diacrylate (45 wt %), and Irgacure TPO-L (5 wt %) without the addition of Peopoly resin and printed using the same procedure (fig. S11).

Technoeconomic analysis

Aspen Plus V11 (Aspen Technology) was used for the lignin-based PSA process simulation (*49*). The universal quasi-chemical activity coefficient (UNIQUAC) model was chosen for the liquid-vapor and liquid-liquid phase behavior (*60*). Most of the components in the simulation were selected directly from the Aspen database. The components not found in the database (i.e., 4-methylguaiacol, 4-ethylguaiacol, 4-propylguaiacol, 4-methylsyringol, 4-ethylsyringol, 4-propylsyringol, guaiacyl methacrylate, 4-methylguaiacyl methacrylate, 4-ethylguaiacyl methacrylate, 4-propylguaiacyl methacrylate, syringyl methacrylate, 4-methylsyringyl methacrylate, 4-ethlysyringyl methacrylate, 4-propylsyringyl methacrylate, and 4-ethylphenyl methacrylate) were defined by their structures, and their physical properties were estimated using the Aspen Plus Property Constant Estimation System (PCES). Lignin was defined with the physical properties reported by the National Renewable Energy Laboratory (*61*). Liquid-vapor equilibrium was essential in modeling these systems, and vapor pressures as a function of temperature were estimated with a combination of experimental data and group contribution methods as described in the Supplementary Materials (see fig. S12 and table S5). Aspen Process Economic Analyzer V11 was used to perform economic evaluations (*50*). Discounted cash flow analysis was conducted, and the MSP, defined as the selling price of the product when the net present value is zero (*62*), was determined for RCD and RD-RCD with three lignin feedstocks. Details on the simulation assumptions, process flow diagrams, and TEA are provided in the Supplementary Materials (see figs. S12 to S19 and tables S5 to S12).

SUPLEMENTARY MATERIALS

Supplementary material for this article is available at https://science.org/doi/10.1126/sciadv.abj7523

REFERENCES AND NOTES

1. W. Schutyser, T. Renders, S. Van den Bosch, S. F. Koelewijn, G. T. Beckham, B. F. Sels, Chemicals from lignin: An interplay of lignocellulose fractionation, depolymerisation, and upgrading. *Chem. Soc. Rev.* **47**, 852–908 (2018).
2. Z. Sun, B. Fridrich, A. De Santi, S. Elangovan, K. Barta, Bright side of lignin depolymerization: Toward new platform chemicals. *Chem. Rev.* **118**, 614–678 (2018).
3. R. Ding, Y. Y. Du, R. B. Goncalves, L. F. Francis, T. M. Reineke, Sustainable near UV-curable acrylates based on natural phenolics for stereolithography 3D printing. *Polym. Chem.* **10**, 1067–1077 (2019).
4. J. S. Mahajan, R. M. O'Dea, J. B. Norris, L. T. J. Korley, T. H. Epps III, Aromatics from lignocellulosic biomass: A platform for high-performance thermosets. *ACS Sustain. Chem. Eng.* **8**, 15072–15096 (2020).
5. R. M. O'Dea, J. A. Willie, T. H. Epps III, 100th anniversary of macromolecular science viewpoint: Polymers from lignocellulosic biomass. Current challenges and future opportunities. *ACS Macro Lett.* **9**, 476–493 (2020).
6. S. Wang, L. Shuai, B. Saha, D. G. Vlachos, T. H. Epps III, From tree to tape: Direct synthesis of pressure sensitive adhesives from depolymerized raw lignocellulosic biomass. *ACS Cent. Sci.* **4**, 701–708 (2018).
7. M. M. Abu-Omar, K. Barta, G. T. Beckham, J. S. Luterbacher, J. Ralph, R. Rinaldi, Y. Román-Leshkov, J. S. M. Samec, B. F. Sels, F. Wang, Guidelines for performing lignin-first biorefining. *Energ. Environ. Sci.* **14**, 262–292 (2021).
8. O. Ajao, M. Benali, A. Faye, H. Li, D. Maillard, M. T. Ton-That, Multi-product biorefinery system for wood-barks valorization into tannins extracts, lignin-based polyurethane foam and cellulose-based composites: Techno-economic evaluation. *Ind. Crops Prod.* **167**, 113435 (2021).
9. B. H. Davison, J. Parks, M. F. Davis, B. S. Donohoe, in *Aqueous Pretreatment of Plant Biomass for Biological and Chemical Conversion to Fuels and Chemicals*, C. E. Wyman, Ed. (John Wiley & Sons Ltd., 2013), pp. 23–36.
10. R. Karinen, K. Vilonen, M. Niemela, Biorefining: Heterogeneously catalyzed reactions of carbohydrates for the production of furfural and hydroxymethylfurfural. *ChemSusChem* **4**, 1002–1016 (2011).
11. D. S. Bajwa, G. Pourhashem, A. H. Ullah, S. G. Bajwa, A concise review of current lignin production, applications, products and their environmental impact. *Ind. Crops Prod.* **139**, 111526 (2019).
12. L. Dessbesell, M. Paleologou, M. Leitch, R. Pulkki, C. Xu, Global lignin supply overview and kraft lignin potential as an alternative for petroleum-based polymers. *Renew. Sustain. Energy Rev.* **123**, 109768 (2020).
13. A. Vishtal, A. Kraslawski, Challenges in industrial applications of technical lignins. *Bioresources* **6**, 3547–3568 (2011).
14. O. Ajao, J. Jeaidi, M. Benali, O. Y. Abdelaziz, C. P. Hulteberg, Green solvents-based fractionation process for kraft lignin with controlled dispersity and molecular weight. *Bioresour. Technol.* **291**, 121799 (2019).
15. O. Ajao, J. Jeaidi, M. Benali, A. Restrepo, N. El Mehdi, Y. Boumghar, Quantification and variability analysis of lignin optical properties for colour-dependent industrial applications. *Molecules* **23**, 377 (2018).
16. N. D. Manke, R. C. Williams, Z. Sotoodeh-Nia, E. W. Cochran, L. Porot, E. Chailleux, S. Pouget, F. Olard, A. J. D. Carrion, J. P. Planche, D. Lo Presti, Performance of a sustainable asphalt mix incorporating high RAP content and novel bio-derived binder. *Road Mater. Pavement* **22**, 812–834 (2021).
17. A. K. Mullick, in *Waste Materials used in Concrete Manufacturing* (William Andrew, Inc., 1996), pp. 352–429.
18. O. Ajao, Lignin bioeconomy: The path forward, *Pulp and Paper Technical Association of Canada—CanmetENERGY*, Webinar (2021); www.paptac.ca/communiques/webinar2-MB-2020.html.
19. M. Benali, O. Ajao, J. Jeaidi, B. Gilani, B. Mansoornejad, in *Production of Biofuels and Chemicals from Lignin* (2016), chap. 13, pp. 379–418.

20. A. Mazar, O. Ajao, M. Benali, N. Jemaa, W. Wafa Al-Dajani, M. Paleologou, Integrated multiproduct biorefinery for furfural production with acetic acid and lignin recovery: Design, scale-up evaluation, and technoeconomic analysis. *ACS Sustain. Chem. Eng.* **8**, 17345–17358 (2020).
21. W. Lan, J. S. Luterbacher, A road to profitability from lignin via the production of bioactive molecules. *ACS Cent. Sci.* **5**, 1642–1644 (2019).
22. C. R. Kumar, N. Anand, A. Kloekhorst, C. Cannilla, G. Bonura, F. Frusteri, K. Barta, H. J. Heeres, Solvent free depolymerization of kraft lignin to alkyl-phenolics using supported NiMo and CoMo catalysts. *Green Chem.* **17**, 4921–4930 (2015).
23. T. Renders, G. Van den Bossche, T. Vangeel, K. Van Aelst, B. Sels, Reductive catalytic fractionation: State of the art of the lignin-first biorefinery. *Curr. Opin. Biotechnol.* **56**, 193–201 (2019).
24. Q. Song, F. Wang, J. Cai, Y. Wang, J. Zhang, W. Yu, J. Xu, Lignin depolymerization (LDP) in alcohol over nickel-based catalysts via a fragmentation–hydrogenolysis process. *Energ. Environ. Sci.* **6**, 994–1007 (2013).
25. T. Renders, S. Van den Bosch, S. F. Koelewijn, W. Schutyser, B. F. Sels, Lignin-first biomass fractionation: The advent of active stabilisation strategies. *Energ. Environ. Sci.* **10**, 1551–1557 (2017).
26. S. Van den Bosch, W. Schutyser, R. Vanholme, T. Driessen, S. F. Koelewijn, T. Renders, B. De Meester, W. J. J. Huijgen, W. Dehaen, C. M. Courtin, B. Lagrain, W. Boerjan, B. F. Sels, Reductive lignocellulose fractionation into soluble lignin-derived phenolic monomers and dimers and processable carbohydrate pulps. *Energ. Environ. Sci.* **8**, 1748–1763 (2015).
27. Y. Liao, S.-F. Koelewijn, G. Van den Bossche, J. Van Aelst, S. Van den Bosch, T. Renders, K. Navare, T. Nicolaï, K. Van Aelst, M. Maesen, H. Matsushima, J. M. Thevelein, K. Van Acker, B. Lagrain, D. Verboekend, B. F. Sels, A sustainable wood biorefinery for low–carbon footprint chemicals production. *Science* **367**, 1385–1390 (2020).
28. W. Lan, J. S. Luterbacher, Preventing lignin condensation to facilitate aromatic monomer production. *CHIMIA Int. J. Chem.* **73**, 591–598 (2019).
29. E. Cooreman, T. Vangeel, K. Van Aelst, J. Van Aelst, J. Lauwaert, J. W. Thybaut, S. Van den Bosch, B. F. Sels, Perspective on overcoming scale-up hurdles for the reductive catalytic fractionation of lignocellulose biomass. *Ind. Eng. Chem. Res.* **59**, 17035–17045 (2020).
30. A. W. Bartling, M. L. Stone, R. J. Hanes, A. Bhatt, Y. Zhang, M. J. Biddy, R. Davis, J. S. Kruger, N. E. Thornburg, J. S. Luterbacher, R. Rinaldi, J. S. M. Samec, B. F. Sels, Y. Román-Leshkov, G. T. Beckham, Techno-economic analysis and life cycle assessment of a biorefinery utilizing reductive catalytic fractionation. *Energ. Environ. Sci.* **14**, 4147–4168 (2021).
31. W. Schutyser, S. Van den Bosch, T. Renders, T. De Boe, S. F. Koelewijn, A. Dewaele, T. Ennaert, O. Verkinderen, B. Goderis, C. M. Courtin, B. F. Sels, Influence of bio-based solvents on the catalytic reductive fractionation of birch wood. *Green Chem.* **17**, 5035–5045 (2015).
32. D. Jacobsen, K. E. McMartin, Methanol and ethylene glycol poisonings. *Med. Toxicol.* **1**, 309–334 (1986).
33. S. Kandasamy, S. P. Samudrala, S. Bhattacharya, The route towards sustainable production of ethylene glycol from a renewable resource, biodiesel waste: A review. *Cat. Sci. Technol.* **9**, 567–577 (2019).
34. M. Hasheminejad, M. Tabatabaei, Y. Mansourpanah, M. K. far, A. Javani, Upstream and downstream strategies to economize biodiesel production. *Bioresour. Technol.* **102**, 461–468 (2011).
35. O. E. Ebikade, N. Samulewicz, S. Xuan, J. D. Sheehan, C. Wu, D. G. Vlachos, Reductive catalytic fractionation of agricultural residue and energy crop lignin and application of lignin oil in antimicrobials. *Green Chem.* **22**, 7435–7447 (2020).
36. C. Cheng, J. Truong, J. A. Barrett, D. Shen, M. M. Abu-Omar, P. C. Ford, Hydrogenolysis of organosolv lignin in ethanol/isopropanol media without added transition-metal catalyst. *ACS Sustain. Chem. Eng.* **8**, 1023–1030 (2020).
37. A. Kloekhorst, Y. Shen, Y. Yie, M. Fang, H. J. Heeres, Catalytic hydrodeoxygenation and hydrocracking of Alcell lignin in alcohol/formic acid mixtures using a Ru/C catalyst. *Biomass Bioenergy* **80**, 147–161 (2015).
38. A. Rahimi, A. Ulbrich, J. J. Coon, S. S. Stahl, Formic-acid-induced depolymerization of oxidized lignin to aromatics. *Nature* **515**, 249–252 (2014).
39. A. Bugarin, B. T. Connell, MgI_2-accelerated enantioselective Morita–Baylis–Hillman reactions of cyclopentenone utilizing a chiral DMAP catalyst. *Chem. Commun.* **46**, 2644–2646 (2010).
40. S. Elangovan, A. Afanasenko, J. Haupenthal, Z. Sun, Y. Liu, A. K. H. Hirsch, K. Barta, From wood to tetrahydro-2-benzazepines in three waste-free steps: Modular synthesis of biologically active lignin-derived scaffolds. *ACS Cent. Sci.* **5**, 1707–1716 (2019).
41. A. W. Bassett, A. E. Honnig, C. M. Breyta, I. C. Dunn, J. F. Stanzione, in *Sustainability & Green Polymer Chemistry Volume 1: Green Products and Processes* (American Chemical Society, 2020), pp. 69–88.
42. D. Ahn, L. M. Stevens, K. Zhou, Z. A. Page, Rapid high-resolution visible light 3D printing. *ACS Cent. Sci.* **6**, 1555–1563 (2020).
43. J. T. Sutton, K. Rajan, D. P. Harper, S. C. Chmely, Lignin-containing photoactive resins for 3D printing by stereolithography. *ACS Appl. Mater. Interfaces* **10**, 36456–36463 (2018).
44. A. L. Holmberg, M. G. Karavolias, T. H. Epps III, Raft polymerization and associated reactivity ratios of methacrylate-functionalized mixed bio-oil constituents. *Polym. Chem.* **6**, 5728–5739 (2015).
45. A. L. Holmberg, N. A. Nguyen, M. G. Karavolias, K. H. Reno, R. P. Wool, T. H. Epps III, Softwood lignin-based methacrylate polymers with tunable thermal and viscoelastic properties. *Macromolecules* **49**, 1286–1295 (2016).
46. A. L. Holmberg, K. H. Reno, N. A. Nguyen, R. P. Wool, T. H. Epps III, Syringyl methacrylate, a hardwood lignin-based monomer for high-T_g polymeric materials. *ACS Macro Lett.* **5**, 574–578 (2016).
47. J. A. Emerson, N. T. Garabedian, D. L. Burris, E. M. Furst, T. H. Epps III, Exploiting feedstock diversity to tune the chemical and tribological properties of lignin-inspired polymer coatings. *ACS Sustain. Chem. Eng.* **6**, 6856–6866 (2018).
48. Adhesives and Sealants Market Size, Share & Trends Analysis Report By Technology, By Product, By Application, By Region (North America, Europe, Asia Pacific, CSA. MEA), and Segment Forecasts, 2019–2025 (*Grand View Research*, 2019).
49. Aspen Plus V11, Aspen Technology, Burlington, MA, 2019.
50. Aspen Economic Analyzer V11, Aspen Technology, Burlington, MA, 2019.
51. H. Wang, X. Bu, Z. Huang, J. Yang, T. Qiu, Synthesis of methacrylic anhydride by batch reactive distillation: Reaction kinetics and process. *Ind. Eng. Chem. Res.* **53**, 17317–17324 (2014).
52. M. Cui, N. A. Nguyen, P. V. Bonnesen, D. Uhrig, J. K. Keum, A. K. Naskar, Rigid oligomer from lignin in designing of tough, self-healing elastomers. *ACS Macro Lett.* **7**, 1328–1332 (2018).
53. E. Feghali, D. J. van de Pas, A. J. Parrott, K. M. Torr, Biobased epoxy thermoset polymers from depolymerized native hardwood lignin. *ACS Macro Lett.* **9**, 1155–1160 (2020).
54. M. Galkin, From stabilization strategies to tailor-made lignin macromolecules and oligomers for materials. *Curr. Opin. Green Sustain. Chem.* **28**, 100438 (2021).
55. K. Van Aelst, E. Van Sinay, T. Vangeel, Y. Zhang, T. Renders, S. Van den Bosch, J. Van Aelst, B. F. Sels, Low molecular weight and highly functional RCF lignin products as a full bisphenol A replacer in bio-based epoxy resins. *Chem. Commun.* **57**, 5642–5645 (2021).
56. R. Vendamme, J. Behaghel de Bueren, J. Gracia-Vitoria, F. Isnard, M. M. Mulunda, P. Ortiz, M. Wadekar, K. Vanbroekhoven, C. Wegmann, R. Buser, F. Héroguel, J. S. Luterbacher, W. Eevers, Aldehyde-assisted lignocellulose fractionation provides unique lignin oligomers for the design of tunable polyurethane bioresins. *Biomacromolecules* **21**, 4135–4148 (2020).
57. O. Ajao, M. Benali, N. El Mehdi, Experimental and computer aided solubility quantification of diverse lignins and performance prediction. *Chem. Commun.* **57**, 1782–1785 (2021).
58. Y. Pu, S. Cao, A. J. Ragauskas, Application of quantitative ^{31}P NMR in biomass lignin and biofuel precursors characterization. *Energ. Environ. Sci.* **4**, 3154–3166 (2011).
59. L. Zhang, C. Shen, R. Liu, GC–MS and FT-IR analysis of the bio-oil with addition of ethyl acetate during storage. *Front. Energy Res.* **2**, 3 (2014).
60. D. S. Abrams, J. M. Prausnitz, Statistical thermodynamics of liquid mixtures: A new expression for the excess gibbs energy of partly or completely miscible systems. *AIChE J.* **21**, 116–128 (1975).
61. R. J. Wooley, V. Putsche, *Development of an Aspen Plus Physical Property Database for Biofuels Components* (National Renewable Energy Laboratory, 1996).
62. A. Athaley, B. Saha, M. Ierapetritou, Biomass-based chemical production using techno-economic and life cycle analysis. *AIChE J.* **65**, e16660 (2019).
63. Y. Nannoolal, J. Rarey, D. Ramjugernath, Estimation of pure component properties. *Fluid Phase Equilib.* **252**, 1–27 (2007).
64. R. L. Brown, S. E. Stein, Boiling point data, in *NIST Chemistry WebBook, NIST Standard Reference Database Number 69*; https://webbook.nist.gov/chemistry/.
65. D. R. Stull, Vapor pressure of pure substances. Organic and inorganic compounds. *Ind. Eng. Chem.* **39**, 517–540 (1947).
66. The Good Scents Company Information System (2021); www.thegoodscentscompany.com/.
67. M. V. Kok, E. Ozgur, Characterization of lignocellulose biomass and model compounds by thermogravimetry. *Energy Sources A Recovery Util. Environ. Eff.* **39**, 134–139 (2017).
68. L. K. J. Tong, W. O. Kenyon, Heats of polymerization. II. Some esters of α-methylacrylic acid. *J. Am. Chem. Soc.* **68**, 1355–1357 (1946).
69. J. F. Stanzione, J. M. Sadler, J. J. La Scala, R. P. Wool, Lignin model compounds as bio-based reactive diluents for liquid molding resins. *ChemSusChem* **5**, 1291–1297 (2012).
70. A. Matherne, US methanol spot prices push higher as production cuts limit regional supplies (ICIS, 2020); www.icis.com/explore/resources/news/2020/08/07/10539057/us-methanol-spot-prices-push-higher-as-production-cuts-limit-regional-supplies [accessed 18 January 2021].
71. S. Wright, Europe glycerine prices slump on oversupply, limited demand (ICIS, 2018); www.icis.com/explore/resources/news/2018/08/02/10247574/europe-glycerine-prices-slump-on-oversupply-limited-demand/ [accessed 15 January 2021].

72. A. Kuznetsov, G. Kumar, M. A. Ardagh, M. Tsapatsis, Q. Zhang, P. J. Dauenhauer, On the economics and process design of renewable butadiene from biomass-derived furfural. *ACS Sustain. Chem. Eng.* **8**, 3273–3282 (2020).
73. Zauba, Import data of methacrylic anhydride; www.zauba.com/import-methacrylic-anhydride-hs-code.html [accessed 16 January 2021].
74. S. Shi, China's butyl acrylate prices to rise on peak turnarounds (ICIS, 2019); www.icis.com/explore/resources/news/2019/02/11/10316656/china-s-butyl-acrylate-prices-to-rise-on-peak-turnarounds/ [accessed 15 January 2021].
75. U.S. Geological Survey, Lime in 2016, *2016 Minerals Yearbook* (2016); www.usgs.gov/media/files/lime-2016-pdf [accessed 18 January 2021].
76. Zauba, Import data of DMAP; www.zauba.com/import-dmap-hs-code.html [accessed 12 January 2021].
77. Alibaba, Pricing of chemicals (2020); http://price.alibaba.com/ [accessed 18 January 2021].
78. F. K. Kazi, A. D. Patel, J. C. Serrano-Ruiz, J. A. Dumesic, R. P. Anex, Techno-economic analysis of dimethylfuran (DMF) and hydroxymethylfurfural (HMF) production from pure fructose in catalytic processes. *Chem. Eng. J.* **169**, 329–338 (2011).
79. BASF, Pricing of precious metals for catalysts; https://apps.catalysts.basf.com/apps/eibprices/mp/YearlyCharts.aspx [accessed 16 January 2021].
80. M. Yang, K. A. Rosentrater, Techno-economic analysis of the production process of structural bio-adhesive derived from glycerol. *J. Clean. Prod.* **228**, 388–398 (2019).
81. D. J. Lundberg, D. J. Lundberg, M. A. Hillmyer, P. J. Dauenhauer, Techno-economic analysis of a chemical process to manufacture methyl-ε-caprolactone from cresols. *ACS Sustain. Chem. Eng.* **6**, 15316–15324 (2018).
82. L. Ao, W. Zhao, Y.-s. Guan, D.-k. Wang, K.-s. Liu, T.-t. Guo, X. Fan, X.-y. Wei, Efficient synthesis of C15 fuel precursor by heterogeneously catalyzed aldol-condensation of furfural with cyclopentanone. *RSC Adv.* **9**, 3661–3668 (2019).
83. M. Hronec, K. Fulajtárova, T. Liptaj, M. Štolcová, N. Prónayová, T. Soták, Cyclopentanone: A raw material for production of C15 and C17 fuel precursors. *Biomass Bioenergy* **63**, 291–299 (2014).
84. Q. Liu, X. Zhang, Q. Zhang, Q. Liu, C. Wang, L. Ma, Synthesis of jet fuel range cycloalkanes with cyclopentanone and furfural. *Energy Fuel* **34**, 7149–7159 (2020).
85. Z. Lin, V. Nikolakis, M. Ierapetritou, Life cycle assessment of biobased p-xylene production. *Ind. Eng. Chem. Res.* **54**, 2366–2378 (2015).
86. Canadian Standards Association (CSA), Kraft lignin—Determination of thermal stability by thermogravimetry, W207:20; www.scc.ca/en/standardsdb/standards/30434.
87. C. A. Cateto, M. F. Barreiro, A. E. Rodrigues, M. C. Brochier-Salon, W. Thielemans, M. N. Belgacem, Lignins as macromonomers for polyurethane synthesis: A comparative study on hydroxyl group determination. *J. Appl. Polym. Sci.* **109**, 3008–3017 (2008).
88. W. Hoareau, W. G. Trindade, B. Siegmund, A. Castellan, E. Frollini, Sugar cane bagasse and curaua lignins oxidized by chlorine dioxide and reacted with furfuryl alcohol: Characterization and stability. *Polym. Degrad. Stab.* **86**, 567–576 (2004).
89. Z. Hu, X. Du, J. Liu, H.-m. Chang, H. Jameel, Structural characterization of pine kraft lignin: Biochoice lignin vs Indulin AT. *J. Wood. Chem. Technol.* **36**, 432–446 (2016).

Acknowledgments

Funding: We are grateful for financial support from the National Science Foundation Growing Convergence Research program (NSF GCR CMMI 1934887) in Materials Life Cycle Management to T.H.E., D.G.V., and M.I. E.R.G. also thanks the Delaware Bioscience Center for Advanced Technology Entrepreneurial Proof of Concept Grant. O.A. and M.B. are grateful for the financial support received from the Program on Energy Research and Development and the Forest Innovation Program of the Canadian Forest Service at Natural Resources Canada. **Author contributions:** Conceptualization: R.M.O., Y.L., E.O.E., E.R.G., O.A., M.B., and T.H.E. Methodology: R.M.O., P.A.P., Y.L., A.A., E.O.E., E.R.G., O.A., and M.B. Investigation and formal analysis: R.M.O., P.A.P., Y.L., A.A., E.O.E., O.A., and M.B. Writing (original draft): R.M.O., P.A.P., and Y.L., Writing (review and editing): R.M.O., P.A.P., Y.L., A.A., E.O.E., E.R.G., O.A., M.B., D.G.V., M.I., and T.H.E. Funding acquisition: O.A., D.G.V., and T.H.E. Supervision: M.B., D.G.V., M.I., and T.H.E. Project administration: T.H.E. **Competing interests:** The authors declare that they have no competing interests. **Data and materials availability:** All data needed to evaluate the conclusions in the paper are present in the paper and/or the Supplementary Materials.

Submitted 30 May 2021
Accepted 22 November 2021
Published 19 January 2022
10.1126/sciadv.abj7523

ScienceAdvances

Ambient-pressure lignin valorization to high-performance polymers by intensified reductive catalytic deconstruction

Robert M. O'DeaPaula A. PrandaYuqing LuoAlice AmitranoElvis O. EbikadeEric R. GottliebOlumoye AjaoMarzouk BenaliDionisios G. VlachosMarianthi IerapetritouThomas H. Epps III

Sci. Adv., 8 (3), eabj7523. • DOI: 10.1126/sciadv.abj7523